# Simultaneous measurement of structure and XUV dielectric constant of nanoscale objects using diffraction of high harmonic radiation

**B Mills[1], C F Chau[2], E T F Rogers[1], J Grant-Jacob[1], S L Stebbings[3], M Praeger[3], A M de Paula[5], C A Froud[6], R T Chapman[4], T J Butcher[1], W S Brocklesby[1], J G Frey[4]**

*[1]Optoelectronics Research Centre, University of Southampton, UK*
*Tel: 023 8059 3718 Email: bem@orc.soton.ac.uk*
*[2]School of Electronics and Computer Science, University of Southampton, UK*
*[3]School of Physics and Astronomy, University of Southampton, UK*
*[4]School of Chemistry, University of Southampton, UK*
*[5]Federal University of Minas Gerais, Brazil*
*[6]Rutherford Appleton Laboratory, UK*

XUV diffraction using radiation generated by high harmonic generation is used simultaneously to determine both the structure and the complex refractive index of a partially ordered array of 196 nm diameter polystyrene spheres.

**OCIS codes:** (340.7480) X-rays, Soft X-rays, Extreme Ultraviolet; (290.4020) Mie Theory

High harmonic generation (HHG) [1-3] has the ability to generate a high flux ($10^{11}$ photons per second per harmonic) of extreme ultraviolet (XUV) radiation in a coherent [4], low divergence beam using a table-top laser source. This combination of flux and coherence allows the source to be used for the study of nanoscale structures by diffraction in regions inaccessible to visible light. In this abstract we describe diffraction in the XUV from ordered 'crystal' arrays of 196 nm polystyrene nanospheres, of the kind often used as templates for photonic or plasmonic crystal structures. From the observed Fraunhofer diffraction we can determine, from a single measurement, both the nanoscale structure and also the XUV complex refractive index.

The sample used is a hexagonal array of polystyrene nanospheres, made by the deposition and evaporation of a weak solution of spheres on a substrate. Scanning electron microscopy (SEM) can be used to determine that the ordering is good across small regions of the samples. However, due to the trade-off of pixel size and scan area inherent in direct imaging, SEM imaging provides less information about lattice ordering than diffraction patterns. Additionally, a non-conducting sample must be coated with a conducting material, such as gold, which irrevocably changes the sample. Diffraction using visible light is not possible because of the small size of the structures – thus XUV diffraction is an ideal technique. In addition to giving information about the ordering of the spheres, XUV diffraction has the added benefit of the capability of measuring the complex refractive index of the nanospheres via measurement of the relative scattering intensities of different diffraction orders. The dielectric constant of materials in the XUV is often obtained by extrapolation of measurements in other spectral regions due to the sub-micron absorption lengths typical in this spectral region. Our experimental scattering results provide a direct measurement of the dielectric constant, which does differ from the extrapolated values in standard tables [5,6].

The XUV radiation used in these experiments is generated by focusing 40fs, ~1mJ pulses of ~800nm radiation into a cell containing argon gas. The typical spectrum generated contains the $23^{rd}$-$33^{rd}$ harmonics of the laser, with fluxes ~$10^8$ photons/harmonic/pulse, in pulses ~10-15fs long. The XUV radiation is separated from the laser using 200 nm thick aluminium filters, and then focused to a ~22 µm spot size on the sample using a Mo/Si multilayer mirror. The XUV focussed spot size can also be varied in order to image the structure across larger regions of the sample. The multilayer mirror strongly reflects three harmonics, and has a peak reflectivity of ~15% for 27.5 nm. The sphere arrays are deposited onto a 50 nm thick silicon nitride window, which is relatively transparent at the XUV wavelengths used. Transmission diffraction patterns are recorded on a XUV CCD camera situated 17 mm from the sample.

Figure 1 shows diffraction intensities recorded from different areas of the sample. The colour scaling is logarithmic. Figure 1(a) shows an area of the sample with few defects. The diffraction pattern is hexagonal, as would be expected for diffraction from a 2-D hexagonal lattice. The individual diffraction spots contain information about both the sample and the incident radiation.

The radial structure that can be seen in figure 1(a) arises from the multiple wavelengths incident on the sample. Each wavelength produces a diffraction pattern whose angular scaling depends on the wavelength, so a radial cross-section gives the spectrum of light incident on the sample. Five harmonics are seen here, limited by the mirror reflectivity. The axial structure arises from small defects in the sample, combined with the phase profile of the XUV at the sample.

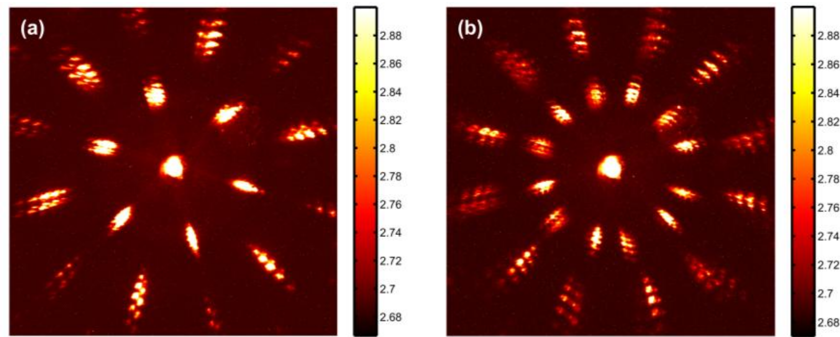


Fig. 1. XUV diffraction patterns for crystal areas with (a) few defects and (b) two well-defined crystallites with axes at different angles

Figure 1(b) shows the diffraction structure in a region where there are two crystallites present within the focussed spot. Two hexagonal diffraction patterns are seen with an angle of ~30° between their axes, indicating the change in the direction of the crystal axes within the nanosphere film. More complex patterns are seen in other sample regions, where ordering is less regular.

The relative intensity of different diffraction orders in figure 1(a) is determined by the form factor of the scattering from the spheres themselves. The form factor can be calculated using Mie theory [7]. The scattering intensities are strongly dependent on the complex refractive index of the material of the spheres, in this case polystyrene. If we pick out one particular wavelength from the multiple wavelength diffraction pattern shown in figure 1(a), we can plot the peak intensities versus diffraction angle and compare that to the predictions from Mie theory. This is shown in figure 2(a) for the 29$^{th}$ harmonic. Excellent agreement is observed for almost four orders of magnitude [8].

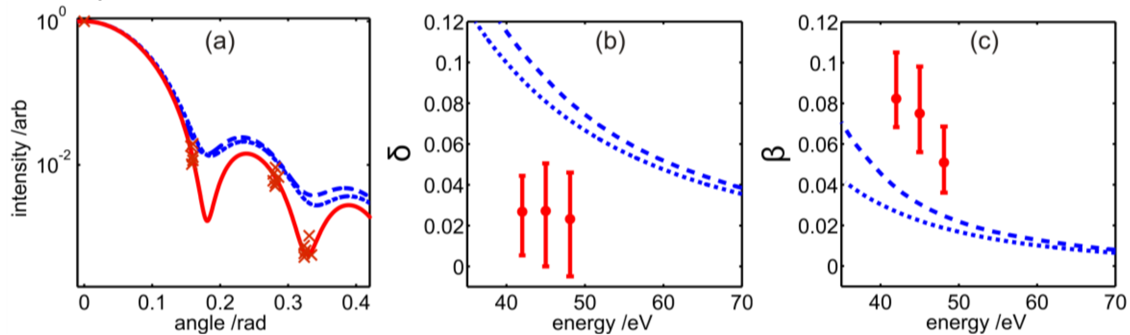


Fig. 2. a) Mie scattering as function of angle, b) real refractive index, c) imaginary refractive index. Solid lines represent experimental results; broken lines correspond to the extrapolated reference databases

As the intensity of different orders is strongly dependent on both the real and imaginary parts of the refractive index of the sphere material, a measurement of the scattering intensities for different harmonics enables the calculation of the complex refractive index as a function of wavelength, usually written as $(1\text{-}\delta) + i\beta$. Figures 2(b) and (c) show the components δ and β as a function of photon energy. The dashed and dotted lines on the figures show the values for δ and β obtained from two of the standard databases of XUV constants, taken from CXRO [5] (blue, dashed) and NIST [6] (blue, dotted). The experimentally measured values (red, solid) are significantly different. Our measurements provide more accurate values than the standard extrapolations.

In summary, we have demonstrated that we can study both the ordering and complex refractive index of nanostructures in the XUV using HHG radiation. In prospect, the ability to perform these experiments on other samples that have absorption edges within the spectrum of the HHG radiation will allow us to look at elemental contrast in ordering, and phase retrieval techniques [9] will allow us to produce direct images of the samples. These experiments illustrate the potential that access to coherent XUV radiation has for simultaneous nanoscale imaging and spectroscopy.

[1] M. Lewenstein, P. Salieres, and A. L'Huillier, Phys. Rev. A 52, 6 (1995)
[2] R. Bartels, S. Backus, E. Zeek, L. Misoguti, G. Vdovin, I. P. Christov, M. M. Murnane, and H. C. Kapteyne, Nature 406, 164 (2000)
[3] P. M. Paul, E. S. Toma, P. Breger, G. Mullot, F. Auge, Ph. Balcou, H. G. Muller, and P. Agostini, Science 292, 1689 (2001)
[4] R. A. Bartels, A. Paul, M. M. Murnane, H. C. Kapteyne, S. Backus, Y. Liu, D. T. Attwood, and C. Jacobson, Science 297, 376 (2002)
[5] B. L. Henke, E. M. Gullikson, and J. C. Davis, Atomic Data and Nuclear Data Tables **54**, 181-342 (1993). Using the interface provided by Centre for X-Ray Optics, http://henke.lbl.gov/optical_constants/getdb2.html [2008, Dec 3]
[6] C.T. Chantler, K. Olsen, R.A. Dragoset, J. Chang, A.R. Kishore, S.A. Kotochigova, and D.S. Zucker. "X-Ray Form Factor, Attenuation and Scattering Tables (version 2.1)". Available at http://physics.nist.gov/ffast [2008, Dec 3]. National Institute of Standards and Technology, Gaithersburg, MD.
[7] C. F. Bohren, and D. R. Huffman, *Absorption and Scattering of Light by Small Particles* (John Wiley & Sons, Weinheim, 2004)
[8] B. Mills, C. F. Chau, E. T. F. Rogers, J. Grant-Jacob, S. L. Stebbings, M. Praeger, A. M. de Paula, C. A. Froud, R. T. Chapman, T. J. Butcher, J. J. Baumberg, W. S. Brocklesby, J. G. Frey. Accepted for publication in Applied Physics Letters
[9] R. L. Sandberg, C. Song, P. W. Wachulak, D. A. Raymondson, A. Paul, B. Amirbekian, E. Lee, A. E. Sakdinawat, C. La-O-Vorakiat, M. C. Marconi, C. S. Menoni, M. M. Murnane, J. J. Rocca, H. C. Kapteyn, and J. Miao, Proc. Natl. Acad. Sci. U.S.A. **105**, 24 (2008)